

Department of Physics and Astronomy  
Experimental Particle Physics Group  
Kelvin Building, University of Glasgow,  
Glasgow, G12 8QQ, Scotland  
Telephone: +44 (0)141 330 2000 Fax: +44 (0)141 330 5881

## Charge sharing in double-sided 3D Medipix2 detectors

D. Pennicard<sup>1</sup>, C. Fleta<sup>1</sup>, G. Pellegrini<sup>2</sup>,  
M. Lozano<sup>2</sup>, J. Marchal<sup>3</sup>, N. Tartoni<sup>3</sup>,  
R. Bates<sup>1</sup>, V. O'Shea<sup>1</sup>, C. Parkes<sup>1</sup>

<sup>1</sup> University of Glasgow, Department of Physics and Astronomy, Glasgow, UK, G12 8QQ

<sup>2</sup> Instituto de Microelectronica de Barcelona, IMB-CNM-CSIC, 08193 Bellaterra, Barcelona, Spain

<sup>3</sup> Diamond Light Source Ltd, Harwell Science and Innovation Campus, Oxfordshire, UK, OX11 0DE

### Abstract

3D detectors are photodiode detectors with n- and p-type electrode columns passing through a silicon substrate. This structure gives a much smaller spacing between the electrodes than in a standard photodiode, greatly reducing the detector's operating voltage and collection time. The device structure also reduces charge sharing between adjacent pixels. This improves the image quality, making these detectors potentially useful for applications such as X-ray diffraction experiments in synchrotrons.

A set of silicon detectors with a simplified "double-sided" 3D structure have been fabricated. After being bump-bonded to Medipix2 single-photon-counting readout chips, they have been tested using X-rays and alpha particles. The test results show that the 3D detectors have substantially lower charge sharing than a planar detector of the same thickness.

*8th International Position Sensitive Detectors Conference  
University of Glasgow, UK, 2008*

# 1 Introduction

A standard silicon photodiode has doped electrodes on the front and back surfaces of a substrate. In a 3D detector [1], these planar electrodes are replaced by sets of electrode columns passing through the substrate. This makes it possible to have an electrode spacing which is up to an order of magnitude smaller than the substrate thickness. The small electrode spacing results in faster charge collection and a greatly reduced depletion voltage.

For X-ray detection, the main attraction of using 3D detectors is their reduced charge sharing between pixels. Firstly, the fast collection speed of the 3D detector means that there is less time for the charge cloud generated by a particle to spread by diffusion. Secondly, the electric field pattern in a 3D detector causes charge carriers to drift away from the pixel boundaries, preventing them from reaching other pixels. In single-photon-counting sensors, this reduced charge sharing can improve the spatial and spectral response [2].

Also, a 3D detector’s fast charge collection and low depletion voltage can counteract the charge trapping and increase in effective doping concentration caused by radiation damage from high-energy hadrons. This means that 3D detectors are potentially useful for future particle physics experiments in high-luminosity colliders [3]. Additionally, the fabrication tools used to produce the electrode columns can also be used to add an “active edge” electrode to the detector array, reducing the insensitive area at the edge of the chip as described in [5].

## 2 Double-sided 3D detectors

The detectors used in this work were designed and fabricated by CNM-IMB (Spain) as described in [6]. They use a “double-sided” 3D structure, with p-type columns extending from the front surface into the silicon which are used for readout, and n-type columns fabricated from the back surface which are connected together and used to bias the detector. The substrate is  $300\mu\text{m}$  thick n-type silicon, and the columns themselves are  $250\mu\text{m}$  long and  $10\mu\text{m}$  in diameter, meaning that neither set of columns passes through the full substrate thickness. Using this “double-sided” structure means that the column fabrication is carried out once on each side, rather than twice on the same side, which makes certain aspects of the fabrication easier. Also, the device can be biased from the backside, rather than requiring extra biasing tracks and contacts on the front surface.

The detectors have a spacing of  $55\mu\text{m}$  between electrodes of the same type, to match the pixel size of Medipix2. Fig. 1 shows the front surface of the detector after fabrication. The tops of the p+ columns are visible. To produce the columns, holes are first etched into the substrate with Deep Reactive Ion Etching (DRIE). Then, the holes are partially filled with doped polysilicon, which also covers the oxide layer on the top surface of the detector. Most of the polysilicon on the surface is etched away, but a square of polysilicon is left around the column, which is then connected to a metal contact. The polysilicon and metal are then passivated, apart from a bump-bond pad used to connect each pixel to the readout chip. The n-electrodes etched from the back surface are placed diagonally between the p-electrodes, forming square pixels. In this first fabrication run, active edges were not included, and so a 3D guard ring was added to collect any surface leakage current.

## 3 3D and Medipix2 single-photon-counting chip

The detectors were bump bonded to Medipix2 [7] readout chips, designed for X-ray detection. These are single-photon counting chips, with a  $256 \times 256$  array of square  $55\mu\text{m}$  pixels. Whenever a hit occurs on a pixel the amplified signal is compared to a pair of adjustable high and low thresholds, and if it falls between the thresholds a counter in the pixel is incremented. At the end of the acquisition period, the counters can be read out. This approach means that the effects of electronic noise are largely eliminated, and the detector has a large, linear dynamic range. However, if charge sharing occurs, any charge-shared hits may be registered in more than one pixel, or missed altogether (depending on the threshold).

In this initial production run, three 3D sensors were bump-bonded. All three were operational, but two had a narrow dead region along one edge, up to about 8 pixels wide, where the pixels were not properly connected to the readout chip. The bump-bonding process requires the chips to be extremely flat, and it’s possible that the polysilicon deposition in the 3D wafer caused the substrate to bend slightly. In the following tests, the third, fully functional chip was used.

A standard, planar Medipix2 sensor, with a  $300\mu\text{m}$ -thick substrate, was also tested for comparison.

During these tests, the detectors were read out via the USB 1.1 interface developed by IEAP-Czech Technical University, Prague [8].

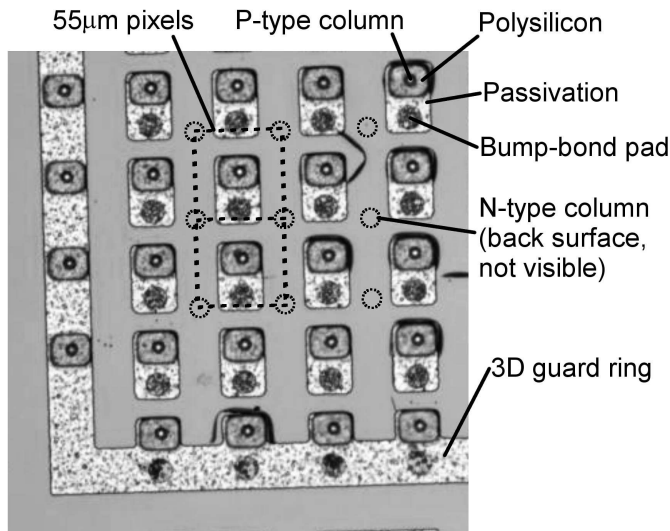


Figure 1: Part of the front surface of the 3D detector before bump bonding to Medipix2. The n-type columns etched from the back are not visible, but the positions of a few have been indicated by circles.

## 4 Spectrum measurement in a synchrotron X-ray beam

The 3D and planar detectors were tested with monochromatic X-rays on beamline B16 at Diamond Light Source. The experimental procedures and results from a variety of tests are reported in [9], along with details on calibration and noise behaviour. Here, just the spectral response results are summarised.

Medipix2 detectors will only register a photon hit if the signal exceeds an adjustable low threshold, THL. (An upper threshold is also available, but it was not used during these tests.) So, by scanning this threshold from above the beam energy down to the noise level, and measuring the change in the count rate at each step, the spectral response of the detector can be found.

The spectral response of the sensors was tested using a monochromatic beam at 12, 15 and 20keV. During the tests the beam profile was kept the same, and the two detectors were moved in and out of the beam, ensuring that the same flux was incident on the two detectors. The 3D detector was biased to 22V, and the planar detector to 100V. (As noted previously, the 3D structure gives a lower depletion voltage.)

Figure 2 shows the results with the 15keV beam. Both detectors show a peak at the beam energy. A Gaussian was fitted to each peak, giving a sigma of around 1keV for each, which will be due to a combination of noise in the individual pixels and threshold dispersion across the detector. However, as well as the peak there are “hits” at lower energies, which occur when the charge from a photon is shared between pixels. It can clearly be seen that the 3D detector has a lower charge-shared signal, and a larger signal peak.

The total numbers of shared and unshared hits on each detector were calculated as indicated in Fig. 2. When a hit is charge-shared between two pixels, one pixel will collect more than half the beam energy and the other will collect less than half. So, only the charge-shared hits above half the beam energy were counted. It was found that 23.4% of the hits on the 3D detector were charge-shared, compared to 39.5% for the planar detector. (These figures are an average of the tests at the three beam energies.) However, the total hit rate seen on the 3D detector was only 86% of that on the planar detector. Since 5% of the device volume is occupied by the columns, increasing to 10% if we include the highly-doped region around each column, the sensitive volume of the 3D detector is expected to be smaller than that of the planar detector. The difference in hit rate could also be partly due to differences in the substrate thicknesses, which are nominally  $300 \pm 15 \mu\text{m}$ .

## 5 Alpha particle tests

As discussed in [10], when an alpha particle hits a silicon detector, it will generate high concentrations of electrons and holes in a small volume near the surface. In addition to the normal drift and diffusion processes occurring during collection, the high carrier concentration means that plasma effects will also occur. Carriers at the outer edge of the cloud will screen out the external electric field, giving carriers within the cloud more time to diffuse. These effects, and the high total energy, mean that the alphas produce large, circular clusters on a detector.

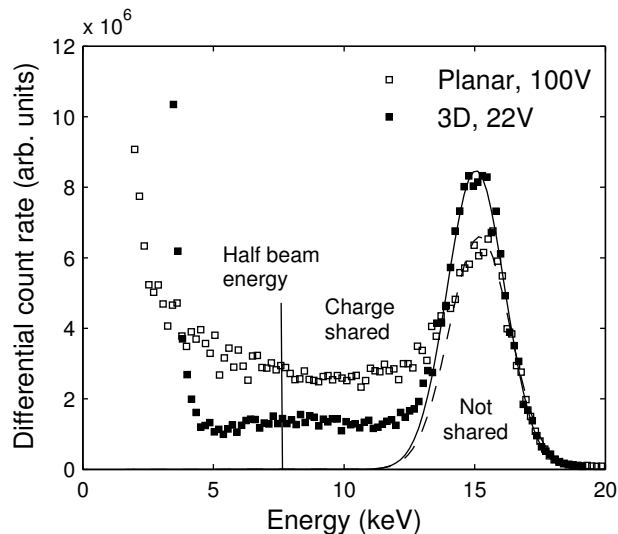


Figure 2: 15keV beam spectra from the 3D and planar detectors. The charge sharing is substantially higher on the planar detector.

Both the 3D and planar detectors were tested using an  $^{241}\text{Am}$  source, which emits 5.637MeV alphas. The source was placed 5mm from the back side of the sensor, to minimise the energy loss of the alphas in air. (Since the front surface of the sensor is bump-bonded to the Medipix2 chip, only the response from the back side could be tested.) The 3D detector was set to 20V, and the planar to 80V. A large number of images were taken with the two sensors, using a short acquisition time to minimise the number of overlapping alpha clusters. Figure 3 shows part of one of these images, containing clusters of different sizes. The number of pixels in each cluster was found, and a histogram of cluster sizes was produced as shown in Fig. 4. Then, a Gaussian fit was applied, and the peak value taken as the typical cluster size. This process was repeated using a range of threshold settings. Note that at lower threshold energies, one- and two-hit clusters due to the gamma emission from  $^{241}\text{Am}$  were also detected; these were excluded from the Gaussian fit.

Figure 5 shows the resulting cluster sizes on the two detectors, at a range of threshold settings. At each threshold setting, the 3D detector shows much smaller cluster sizes, demonstrating its reduced charge sharing. Because the alpha particle is deposited at the back surface of the detector, and the planar detector collects the charge at the front surface, the difference in collection distance between the 3D and planar detectors will be particularly dramatic in this case. Also, in addition to the 3D detector's fast collection time and the self-shielding effect of its electric field pattern, the 3D electrodes could perhaps disrupt the plasma effects occurring in the charge cloud. Both detectors show a fairly similar drop in cluster size as the threshold is increased, because using a high threshold will exclude the pixels at the outer edges of the charge cloud.

## 6 Conclusions

A set of Medipix2 double-sided 3D sensors have been successfully fabricated and tested. Tests using both X-rays and alpha particles have shown that the detector gives significantly less charge sharing than a planar detector of the same pixel size and substrate thickness.

## Acknowledgements

This work has been supported by the Spanish Ministry of Education and Science through the GICSERV program "Access to ICTS integrated nano- and microelectronics cleanroom". This work was carried out in the context of the RD50 collaboration.

## References

- [1] S. I. Parker, C. J. Kenney, J. Segal, Nucl. Instr. and Meth. A 395 (3) (1997) 328–343.
- [2] M. Chmeissani, B. Mikulec, Nucl. Instr. and Meth. A 460 (1) (2001) 81–90.

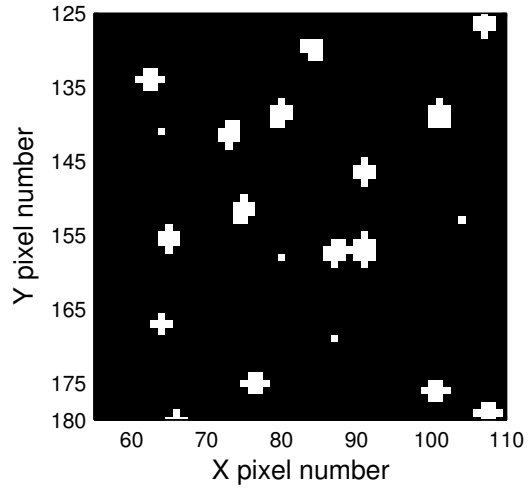


Figure 3: Part of an image of alpha clusters, taken on the 3D detector with the threshold at 10keV. At this low threshold, single-pixel hits due to gammas can also be seen.

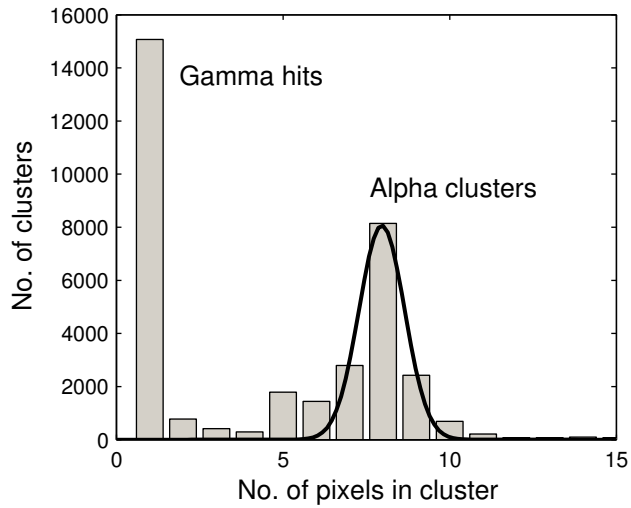


Figure 4: Histogram of alpha cluster sizes seen on the 3D detector, with the threshold set to 10keV. A Gaussian fit has been applied to the alpha cluster distribution, to find the typical cluster size.

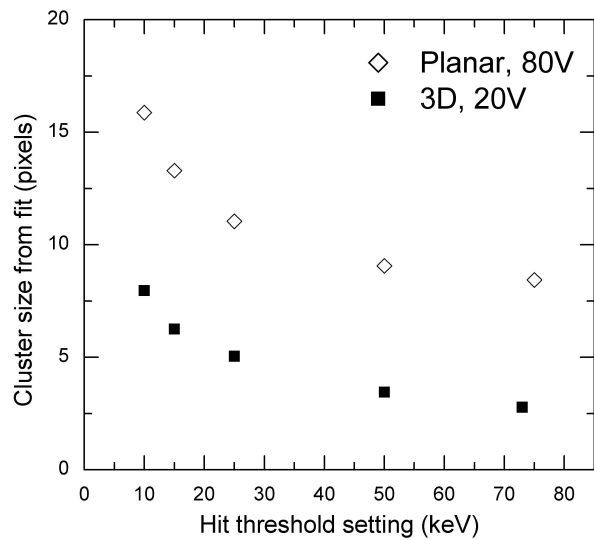


Figure 5: Variation in alpha cluster size with threshold setting for the 3D and planar detectors. The smaller clusters on the 3D detector show that it has lower charge sharing.

- [3] C. Da Via, G. Anelli, J. Hasi, P. Jarron, C. Kenney, A. Kok et al., Nucl. Instr. and Meth. A 509 (1–3) (2003) 86–91.
- [4] C. Kenney, S. Parker, J. Segal, C. Storment, IEEE Trans. Nucl. Sci. 46 (4) (1999) 1224–1236.
- [5] C. J. Kenney, S. I. Parker, B. Krieger, B. Ludewigt, T. P. Dubbs, H. Sadrozinski, IEEE Trans. Nucl. Sci. 48 (2) (2001) 189–193.
- [6] G. Pellegrini, M. Lozano, M. Ullan, R. Bates, C. Fleta, D. Pennicard, Nucl. Instr. and Meth. A 592 (1–2) (2008) 38–43.
- [7] X. Llopart, M. Campbell, R. Dinapoli, D. S. Segundo, E. Pernigotti, IEEE Trans. Nucl. Sci. 49 (5) (2002) 2279–2283.
- [8] Z. Vykydal, J. Jakubek, S. Pospisil, Nucl. Instr. and Meth. A 563 (1) (2006) 112–115.
- [9] D. Pennicard, J. Marchal, C. Fleta, G. Pellegrini, M. Lozano, C. Parkes et al., Submitted to J. Synchrotron Radiat.
- [10] M. Campbell, E. Heijne, T. Holy, J. Idarraga, J. Jakubek, C. Lebel et al., Nucl. Instr. and Meth. A 591 (1) (2008) 38–41.